

**Probing the effective mass anisotropy of  $\Gamma$  electrons in a GaAs/(AlGa)As quantum well**

E. E. Vdovin,<sup>1</sup> Yu. N. Khanin,<sup>1</sup> Yu. V. Dubrovskii,<sup>1</sup> P. C. Main,<sup>2</sup> L. Eaves,<sup>2</sup> M. Henini,<sup>2</sup> and G. Hill<sup>3</sup>  
<sup>1</sup>*Institute of Microelectronics Technology and High Purity Material, Russian Academy of Sciences, Chernogolovka, Moscow District, 142432 Russia*

<sup>2</sup>*School of Physics and Astronomy, University of Nottingham, Nottingham, NG7 2RD, United Kingdom*

<sup>3</sup>*Department of Electronic and Electrical Engineering, University of Sheffield, Sheffield S3 3JD, United Kingdom*

(Received 25 November 2002; published 6 May 2003)

We use resonant magnetotunneling spectroscopy to probe the band structure of the lowest-energy electron subband of a GaAs (001) quantum well, embedded in a resonant tunneling diode. A magnetic field,  $B$ , is applied perpendicular to the tunneling direction. The amplitude and bias position of the resonant peaks in the tunnel current are sensitive to both the magnitude and orientation of  $B$  relative to the crystalline axes. Consistent with earlier work, the axis of the anisotropy rotates by  $90^\circ$  on reversing the bias direction, as a result of interface band mixing. By incorporating a single atomic layer of InAs into the quantum well we can modify the eigenfunction of the lowest subband and hence control and investigate the nature of the band anisotropy.

DOI: 10.1103/PhysRevB.67.205305

PACS number(s): 71.18.+y, 73.40.Gk, 73.61.Ey, 73.21.-b

**I. INTRODUCTION**

The precise form of the band structure of GaAs close to the  $\Gamma$  point of the Brillouin zone has been the focus of much attention, most recently in connection with the stripe phases of the quantum Hall effect.<sup>1</sup> Several experimental studies of the band structure have been concerned with a determination of the in-plane effective mass of electrons confined in GaAs/(AlGa)As quantum wells (QWs) and its dependence on the QW width.<sup>2</sup> However, such experiments are not sensitive to any anisotropy of the effective mass. Recently, there have been reports of an axial effective-mass anisotropy for  $\Gamma$  electrons in QWs (Refs. 3–5) grown on (001) planes. The experiments involved the technique of resonant magnetotunneling spectroscopy, in which electrons tunnel perpendicular to the plane of the QW. A similar procedure has been used to probe the conduction-band<sup>6</sup> and valence-band anisotropies at high energies in a wide quantum well.<sup>7</sup> The voltage at which a particular resonance occurs is a measure of the energy of the state into which the electron is tunneling. By applying a magnetic field,  $B$ , in the plane of the quantum well, the tunneling electrons are given an in-plane component of momentum, due to the action of the Lorentz force. Since momentum is conserved in the tunneling process, by varying the direction of the in-plane  $B$ , the dispersion curve of the electrons may be investigated by monitoring how the bias voltage at which a particular resonance occurs depends on the magnitude and direction of the magnetic field.

The origin of the axial anisotropy may be explained qualitatively in terms of a difference in the band mixing that occurs, respectively, at the GaAs/(AlGa)As and (AlGa)As/GaAs interfaces on each side of the QW.<sup>5</sup> The important asymmetry is that the Al-As (or the Ga-As) bond planes at the two sides of the QW have orthogonal [110] and [ $\bar{1}\bar{1}0$ ] orientations. Figure 1 shows schematically the arrangement of atoms for an AlAs/GaAs interface, but similar remarks apply to the Al<sub>0.4</sub>Ga<sub>0.6</sub>As/GaAs interface of the type occurring in our samples. Assuming ideal interfaces, with no bias applied to the resonant tunneling diode in which the QW is confined, the two directions are equivalent. However, when a

voltage is applied, the electric field breaks the symmetry, due to the polar character of the bonds. At one interface, for example, the field pushes electrons closer to the first plane of Ga atoms in the well and away from the first plane of As atoms in the barrier. At the opposite interface, where the bonds have a different orientation, the electrons are forced towards the As atoms. Experimentally, there are two principal effects of the bias. One is to alter the polarization of the bond, thereby increasing the anisotropy. The second effect is to push the peak of the envelope function of the QW state closer to one of the interfaces, depending on the sign of the bias. Therefore, the measured anisotropy depends on both the magnitude and the sign of the applied voltage.<sup>5</sup>

In this paper, we further investigate the origin of the anisotropy effect by engineering the form of the envelope wave function of the electrons in the QW. This is achieved by the introduction of a thin InAs layer at various positions within the GaAs QW. By placing the layer in the center of the well, we are able to increase the localization of the electrons at the center of the QW, reducing the probability density at the interfaces. In this case, we do not observe the reversal of the anisotropy on changing the bias direction, although we still see the well-established, fourfold anisotropy of the  $\Gamma$ -conduction band, typical of zinc-blende semiconductors. In contrast, when the InAs layer is close to one of the barriers, the envelope function is compressed closer to that interface. The measurements show axial anisotropy, similar to that seen in samples without an InAs layer, but the form is not dependent on the sign of the applied bias. Consequently, we are able to control the strength of the band mixing by embedding an InAs layer at different positions in the QW.

**II. SAMPLES**

All devices were resonant tunneling diodes (RTDs) grown by molecular-beam epitaxy on  $n^+$ -doped, (001) GaAs substrates. There are three types of structures, which we label A, B, and C. Type A was a conventional RTD, with a 11.2-nm GaAs QW sandwiched between two, 8.3-nm-wide Al<sub>0.4</sub>Ga<sub>0.6</sub>As barriers. Two nominally undoped 50-nm spacer

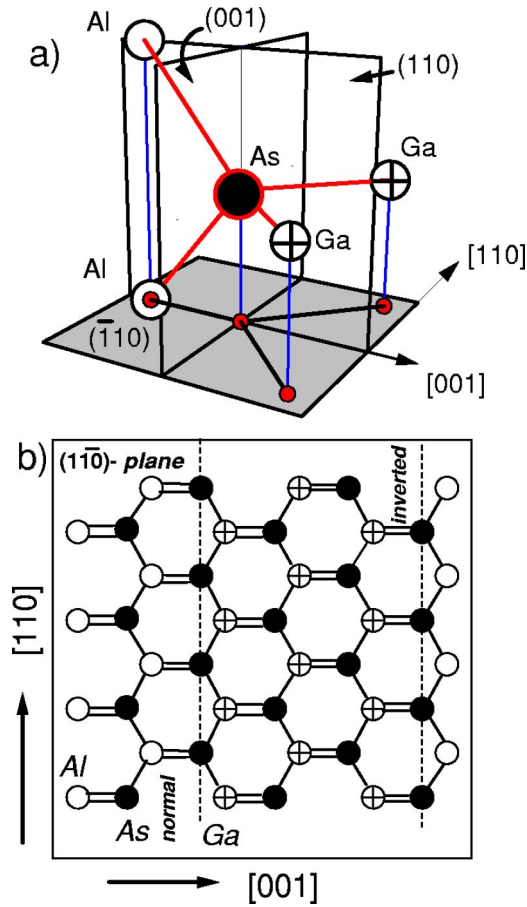


FIG. 1. (a) Tetrahedral bonding at the normal AlAs/GaAs interface (GaAs on AlAs). The Al-As bonds lie in the (110) plane and the Ga-As bonds lie in the (110) plane. With the projection on the (110) plane Ga, Al, and As atoms are indicated by small closed circles. At an inverted interface these planes are interchanged. (b) The bonding arrangement in an AlAs/GaAs/AlAs quantum well, with the projection on the (110) plane.

layers separate the barriers from graded  $n$ -type contact regions, with the donor concentration increasing from  $2 \times 10^{17} \text{ cm}^{-3}$  to  $3 \times 10^{18} \text{ cm}^{-3}$ . Type B devices were of the same basic structure except that a thin wetting layer (WL) of InAs was incorporated in the QW, close to the (AlGa)As/GaAs interface. The WL had a width of 1 monolayer, smaller than the critical thickness for the formation of self-assembled quantum dots.<sup>8</sup> In type C structures, the WL was at the center of the QW. Details of devices B and C are given in the Table I. For all the devices, ohmic contacts were produced by successive deposition of AuGe, Ni, and Au layers with subsequent annealing. Mesas, with diameters between  $50 \mu\text{m}$  and  $200 \mu\text{m}$ , were fabricated using conventional optical lithography and chemical etching.

Figure 2 shows the conduction-band profile for each of the samples with an applied bias of  $V=300 \text{ mV}$ . At this bias, due to the presence of the spacer layer between the contacts and the QW, a two-dimensional electron gas forms at the emitter barrier. Also shown in the figure are the results of self-consistent calculations of the wave function of the electronic ground state of the QW, obtained using the Schrödinger

TABLE I. Layer composition of devices.

Material	Sample B	Sample C	Doping ( $\text{cm}^{-3}$ )
GaAs	$0.3 \mu\text{m}$	$0.3 \mu\text{m}$	$3 \times 10^{18}$
GaAs	50 nm	50 nm	$2 \times 10^{17}$
GaAs	50 nm	50 nm	undoped
$\text{Al}_{0.4}\text{Ga}_{0.6}\text{As}$	8.3 nm	8.3 nm	undoped
GaAs	1 nm	5.5 nm	undoped
InAs	0.3 nm	0.3 nm	undoped
GaAs	10 nm	5.5 nm	undoped
$\text{Al}_{0.4}\text{Ga}_{0.6}\text{As}$	8.3 nm	8.3 nm	undoped
GaAs	50 nm	50 nm	undoped
GaAs	50 nm	50 nm	$2 \times 10^{17}$
GaAs	$0.3 \mu\text{m}$	$0.3 \mu\text{m}$	$3 \times 10^{18}$
GaAs	substrate	substrate	$3 \times 10^{18}$

inger and Poisson equations. A self-consistent solution of the nonlinear system of Schrödinger-Poisson equations is obtained by a numerical method which is similar to that described in Ref. 9. The presence of the InAs WL modifies the electronic structure of the QW by creating a deep and narrow well, in addition to the broader GaAs QW formed by the two (AlGa)As barriers. In sample A [Fig. 2(a)], at  $V=300 \text{ mV}$ , the ground-state wave function is displaced slightly to the right; the amplitude of the wave function is about twice as large at the right-hand interface as it is at the left. For sample B [Fig. 2(b)], the wave function is compressed against the emitter interface, despite the effect of the applied voltage. Finally, Fig. 2(c) shows that, for type C devices, the ground-state wave function is localized much closer to the center of the well than in type A and the applied bias has only a small effect on the relative amplitudes of the wave function at the two interfaces.

Figure 3(a) shows the wave functions, at zero bias, of the first two electronic states for a QW with the wetting layer close to the left-hand barrier. We have also calculated the energies of the first three electronic states as a function of the position of the WL in the QW [Fig. 3(b)]. It is easy to understand the energy dependence qualitatively. For the ground state, the total energy is lowest when the potential minimum is at the center of the QW, where the wave function has maximum amplitude. In contrast, for the first excited state, when the WL is at the center of the QW, the energy is almost the same as in the unperturbed QW, because the wave function has a node. Note that, for sample C, where the WL is at the center of the well, the ground-state energy is below the GaAs conduction-band edge. This means that, at zero bias, the lowest-energy subband of the quantum well is populated by electrons so that it is in resonance with electrons occupying states in the heavily doped contact layer in zero magnetic field. In contrast, for samples A and B, the energies of the ground state are well above the band edge and it is necessary to apply a bias of about  $100 \text{ mV}$  to bring the lowest-energy subband of the well into resonance.

### III. EXPERIMENT

We use resonant magnetotunneling spectroscopy to probe the in-plane dispersion  $E(k_{\parallel})$  of electrons in the QW. At a

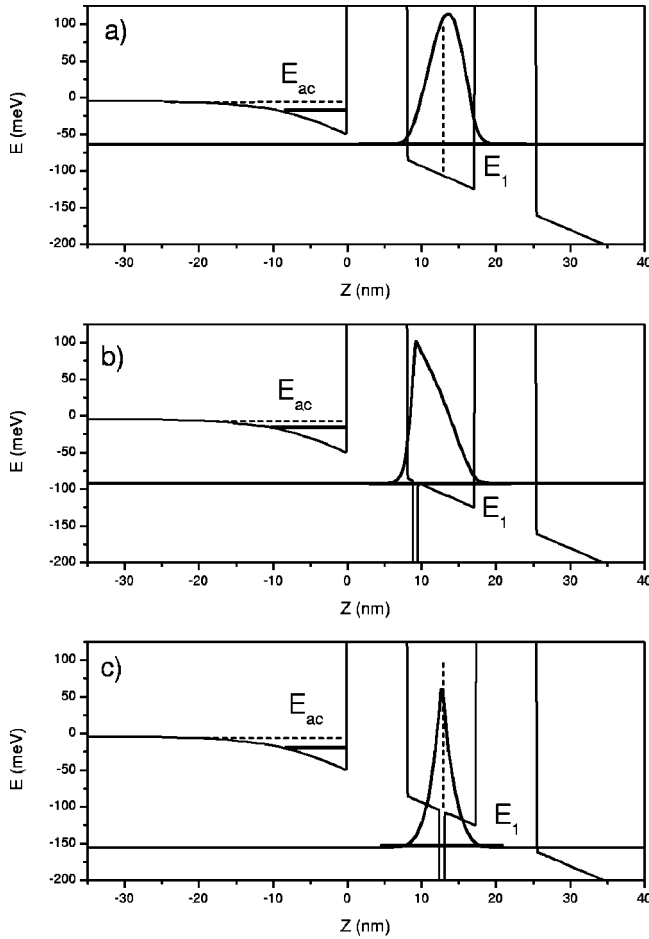


FIG. 2. The conduction-band profile and the probability density  $|\Psi|^2$  of the wave functions of the lowest-energy  $E_1$  electronic QW subband: (a) the control sample A; (b) sample B, with an InAs layer near the (AlGa)As/GaAs interface; and (c) sample C, with an InAs layer in the center of the GaAs QW, calculated using the Schrödinger and Poisson equations at bias  $V=300$  mV.

particular voltage,  $V_p$ , electrons in the contacts will be resonant with a state in the well and there will be a peak in  $I(V)$ . When a magnetic field,  $B$ , is applied in the plane of the well, electrons tunneling into the well over a distance  $\Delta s$  acquire an in-plane momentum component  $\Delta k_{\parallel} = eB\Delta s/\hbar$  in the direction perpendicular to the magnetic field due to the action of the Lorentz force. In the absence of scattering, momentum is conserved. In general, the voltage at which the resonant peak occurs will change by an amount  $\Delta V_p$ , which is approximately proportional to  $E(k_{\parallel})$ . In other words, the extra energy acquired by the electron as a result of its in-plane motion means that more voltage is required to reach resonance. By rotating the direction of  $B$  in the plane of the QW, it is possible to investigate any anisotropy of the band structure in the (001) plane.

Figure 4(a) shows the  $I(V)$  characteristics at 4.2 K for sample B in magnetic fields up to 7 T, applied parallel to a [100] direction in the plane of the QW. The effect of the magnetic field is to broaden the resonance and shift it to higher bias. The shift in voltage,  $\Delta V_p$ , varies approximately as  $B^2$  [Fig. 4(b)], consistent with a parabolic dispersion re-

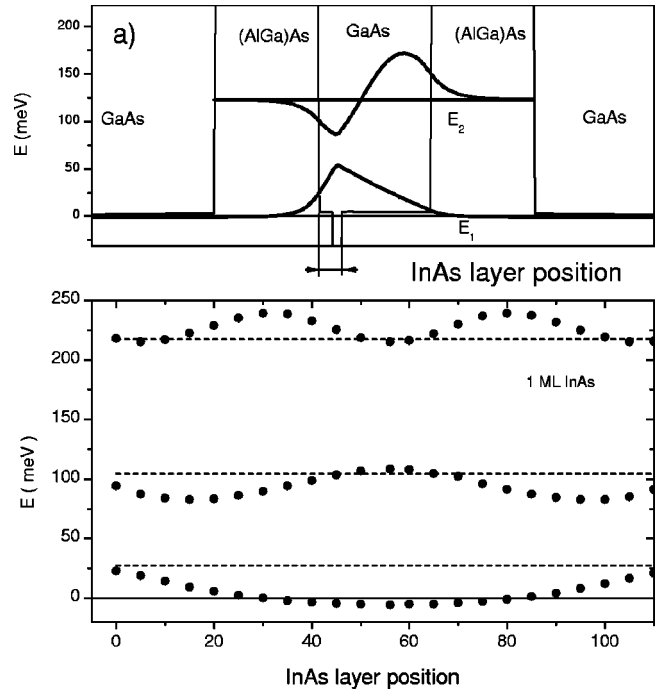


FIG. 3. (a) The conduction-band profile and wave functions of the  $E_1$  electronic states of the samples with an InAs layer close to an interface. (b) The calculated energy of the QW quasibound states as a function of the position of the InAs layer for a 11-nm GaAs/AlGaAs QW with a layer of thickness  $WL=1$  ML. The dashed lines show the energy of the QW quasibound states for an 11-nm GaAs/AlGaAs QW without an InAs layer.

lation for electrons in the well, since  $\Delta k_{\parallel} \sim B$ .

When  $B$  is rotated, both the magnitude of the peak current values  $I_p$  and  $V_p$  change in a correlated manner, i.e., the directions associated with larger currents also correspond to

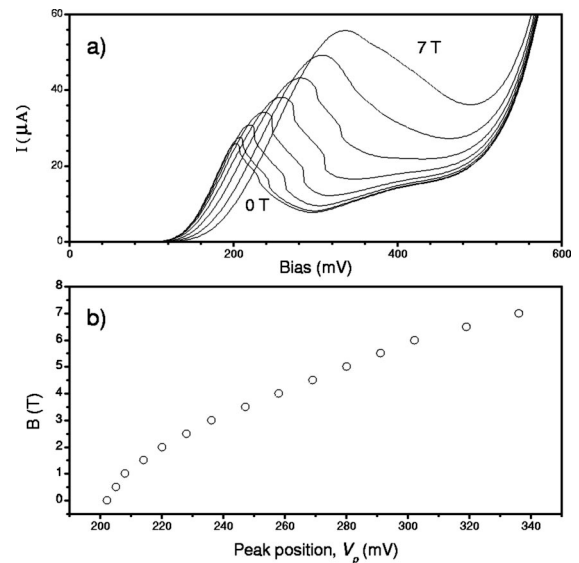


FIG. 4. (a)  $I(V)$  characteristics of sample B as a function of magnetic field from zero to  $B = 7$  T, with steps of 1 T, applied parallel to a [100] direction in the plane of the quantum well. (b) Peak position plotted vs  $B$ .

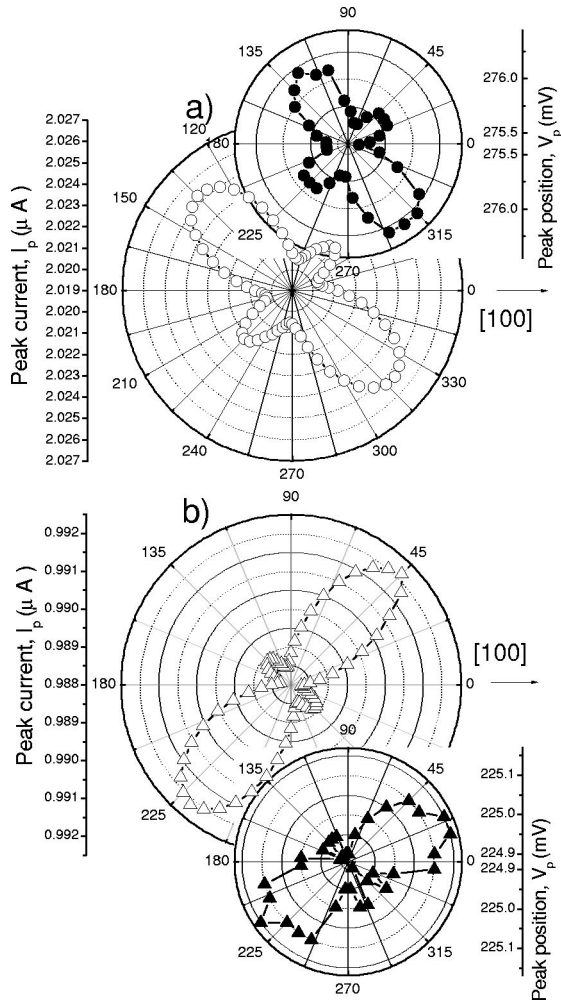


FIG. 5. Polar plot of the peak current and the peak position of the control sample A for the  $E1$  resonance, as the field is rotated in the plane of the interface. Magnetic fields of 5 T were applied in the (a) forward and (b) reverse bias directions, respectively.

larger voltage shifts. Generally, however, the current is a more sensitive probe of the anisotropy than is the bias shift.<sup>4,5,10</sup> Typical experimental data for sample A, for the variation of the voltage position and the peak current with the direction of magnetic field at 5 T, are shown as polar plots in Fig. 5, in both forward and reverse biases. A maximum current modulation  $\Delta I/I$  of about  $\sim 0.4\%$  is observed, with a clear, twofold anisotropy observed for both bias directions. The anisotropy of the voltage position has a similar magnitude, indicating a corresponding anisotropy in the effective mass. Note that the principal axis of the anisotropy is different for the two bias directions, rotating by  $90^\circ$  as the voltage is reversed.

In Fig. 5,  $0^\circ$  corresponds to a  $[100]$  direction, so the principal axes for the anisotropy are oriented along the  $\langle 110 \rangle$  directions. Furthermore, as reported by Reker *et al.*,<sup>5</sup> the principal axes for the two bias directions are orthogonal to each other. These plots reflect the variation of electron energy at constant  $k_{\parallel}$  and hence show that the constant energy surface of the QW subband is anisotropic, with the principal axes along the  $\langle 110 \rangle$  directions, consistent with the orthogo-

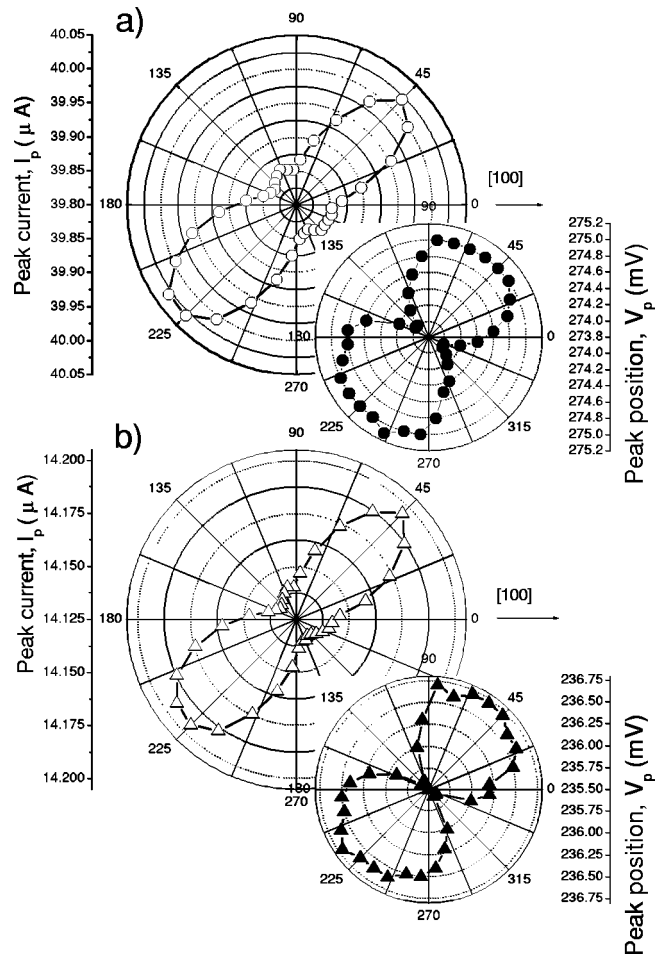


FIG. 6. The peak current and peak position vs in-plane magnetic field direction for sample B for the  $E1$  resonance. Magnetic fields of 5 T were applied in the (a) forward and (b) reverse bias directions, respectively.

nal orientation of bond planes at opposite interfaces in the QW. As discussed above, the effect of changing the bias is to push the ground-state wave function to one of the interfaces depending on the sign of  $V$ .

Figure 6 shows similar polar plots for sample B, in which a WL is embedded in the QW, close to the (AlGa)As/GaAs interface. Again, there is a pronounced twofold anisotropy but, in this case, the direction of the bias has no effect on the orientation of the principal axis. The results may be understood in terms of Fig. 2(b). The effect of the WL is to compress the wave function close to one of the interfaces. An applied bias of 300 mV has little effect on this compression, so one would not expect to see any change in the anisotropy on reversing the bias. For both voltage directions, the anisotropy is that of the (AlGa)/GaAs interface. However, it is necessary to apply some bias to induce the band anisotropy between the two crystallographic directions.

The results for sample C, where the InAs WL is in the center of the sample, are shown in Fig. 7. For this sample, in zero magnetic field, the ground state is occupied and resonant tunneling occurs around zero bias. However, at 8 T, the resonance peak has shifted to about 150 mV. As in the other two cases, the zero of the angular scale corresponds to the

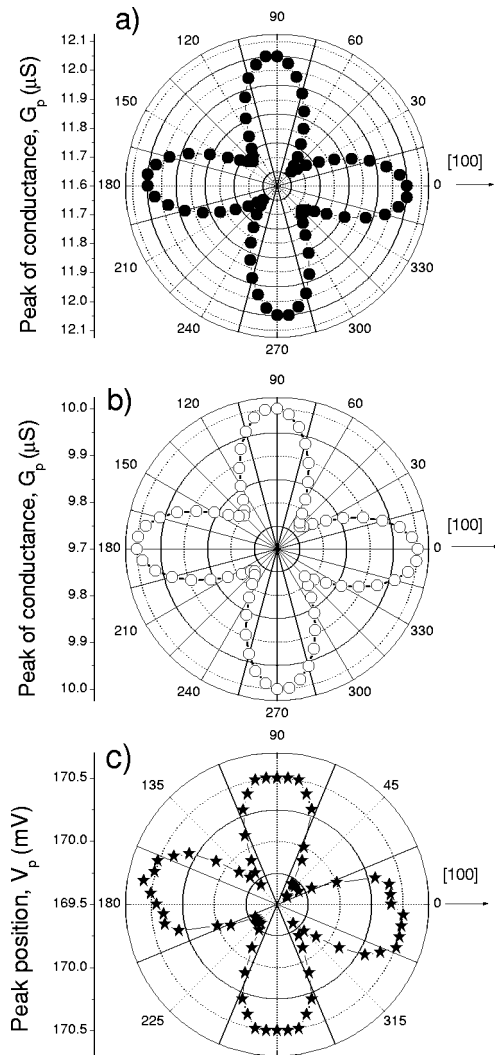


FIG. 7. Dependence of the peak in conductance and the peak position vs in-plane magnetic-field direction for sample C for the  $E1$  resonance. Magnetic fields of 8 T were applied in the (a) and (c) forward and (b) reverse bias directions, respectively.

magnetic field oriented along a  $[100]$  direction. There are three principal features in the anisotropy for this case relative to samples A and B. First, the anisotropy has a fourfold symmetry instead of the axial symmetry of the two other cases. Second, the principal axes are  $[100]$  and  $[010]$ , instead of  $[110]$  and  $[\bar{1}10]$  as for A and B. Finally, the pattern is the same in forward and reverse biases. Similar remarks apply for all values of applied magnetic field.

Unlike sample B, where the positioning of the WL introduces an intrinsic asymmetry into the device, in sample C the

WL is at the center of the QW. Therefore, we attribute the lack of dependence of the anisotropy on bias direction to the localization of the ground-state electronic wave function, as shown in Fig. 2(c). Even with 300 mV applied, there is no significant shift of the peak of the wave function from the center of the QW. Figure 2(c) also shows that the amplitude of the wave function is very small at the interfaces, particularly compared with the case for that of sample A. Therefore, it is likely that the interfaces will have a much smaller effect on the in-plane dispersion than that in the other two cases, and that the anisotropy observed for sample C is due to a bulk effect. The fourfold symmetry of the anisotropy, with principal axes corresponding to the sides of the cubic unit cell, is also consistent with theoretical predictions<sup>11</sup> of the magnitude of the effective-mass anisotropy close to the  $\Gamma$  point in bulk GaAs. We therefore argue that, for samples in which a WL is placed at the center of the QW, the observed anisotropy of the dispersion relation reflects that of bulk GaAs and is not related to the interfaces at all. Comparable results were obtained by Hughes *et al.*,<sup>6</sup> who performed a similar experiment using a wide (120 nm) QW without an InAs layer. Figure 7(c) shows the anisotropy of the bias position, which has the same symmetry as the conductance. The anisotropy of the effective mass is  $\sim 0.5\%$ .

In summary, we see a small  $\langle 110 \rangle$  twofold anisotropy relative to the direction of B, similar to that reported in Ref. 5, for sample A. This anisotropy can be understood by the orthogonal  $\langle 110 \rangle$  orientation of bond planes at opposite interfaces of the quantum well. For sample B, in which a wetting layer of InAs is embedded near the (AlGa)As/GaAs interface, we also observe two-fold anisotropy. However, in this case, the principal axis of anisotropy did not rotate upon reversing the bias. The wave function in sample B is confined close to one of the (AlGa)As/GaAs interfaces for both bias polarities and, as a result, the observed anisotropy reflects only the band mixing at this interface. A fourfold anisotropy, spanned by the  $[100]$  and  $[010]$  directions, was observed for sample C, in which a wetting layer of InAs is embedded in the central plane of the GaAs QW. These data reflect the  $\Gamma$ -minimum anisotropy of the GaAs QW and are not related to the interface.

## ACKNOWLEDGMENTS

The work was partly supported by RFBR (Grant No. 03-02-17693), INTAS (Grant No. 01-2362), and EPSRC (United Kingdom). E.E.V. and Y.V.D. gratefully acknowledge support from the Royal Society. We are grateful to V.V. Belov for technical assistance and to V. Sirotkin for assistance with the self-consistent calculations.

<sup>1</sup>M. P. Lilly, K. B. Cooper, J. P. Eisenstein, L. N. Pfeiffer, and K. W. West, *Phys. Rev. Lett.* **82**, 394 (1999).

<sup>2</sup>See, for example, R. J. Warburton, J. G. Michels, R. J. Nicholas, J. J. Harris, and C. T. Foxon, *Phys. Rev. B* **46**, 13 394 (1992).

<sup>3</sup>T. Reker, H. Im, H. Choi, L. E. Bremme, Y. C. Chung, R. Grey,

G. Hill, and P. C. Klipstein, in *Proceedings of the International Conference on the Physics of Semiconductors, Osaka, 2000*, edited by N. Miura and T. Ando (Springer, Berlin, 2001), p. 827.

<sup>4</sup>E. E. Vdovin, Yu. N. Khanin, A. V. Veretennikov, A. Levin, A. Patane, Yu. V. Dubrovskii, L. Eaves, P. C. Main, M. Henini, and

- G. Hill, Pis'ma Zh. Éksp. Teor. Fiz. **74**, 43 (2001) [JETP Lett. **74**, 41 (2001)].
- <sup>5</sup>T. Reker, H. Im, L. E. Bremme, H. Choi, Y. Chung, P. C. Klipstein, and Hadas Shtrikman, Phys. Rev. Lett. **88**, 056403 (2002).
- <sup>6</sup>O. H. Hughes, M. Henini, E. S. Alves, M. L. Leadbeater, L. Eaves, M. Davies, and M. Heath, J. Vac. Sci. Technol. B **7**, 1041 (1989).
- <sup>7</sup>R. K. Hayden, D. K. Maude, L. Eaves, E. C. Valadares, M. Henini, F. W. Sheard, O. H. Hughes, J. C. Portal, and L. Cury, Phys. Rev. Lett. **66**, 1749 (1991); R. K. Hayden, E. C. Valadares, M. Henini, L. Eaves, D. K. Maude, and J. C. Portal, Phys. Rev. B **46**, 15 586 (1992).
- <sup>8</sup>J.-Y. Marzin, J.-M. Gerard, A. Izrael, D. Barrier, and G. Bastard, Phys. Rev. Lett. **73**, 716 (1994).
- <sup>9</sup>H. Tan, G. L. Snider, L. D. Chang, and E. L. Hu, J. Appl. Phys. **68**, 4071 (1990). In our method for greater computational efficiency we use meshes adapted to behaviors of the system solution and special guesses calculated in the Thomas-Fermi approximation [for details see V. Sirotkin (to be published)].
- <sup>10</sup>U. Gennser, V. P. Kesan, D. A. Syphers, T. P. Smith, III, S. S. Iyer, and E. S. Yang, Phys. Rev. Lett. **67**, 3828 (1991).
- <sup>11</sup>U. Rossler, Solid State Commun. **49**, 943 (1984).